Sound velocities in highly-oriented pyrolytic graphite shocked to 18 GPa: orientational order dependence and elastic instability

Marcel Lucas, J. M. Winey, and Y. M. Gupta

Institute for Shock Physics and Department of Physics, Washington State University, Pullman, Washington 99164, USA

19 April 2024 13:09:15

ABSTRACT

Previous reports of rapid phase transformation above 18 GPa [Erskine and Nellis, Nature **349**, 317 (1991)] and large elastic waves below 18 GPa [Lucas *et al.*, J. Appl. Phys. **114**, 093515 (2013)] for shock-compressed ZYB-grade highly-oriented pyrolytic graphite (HOPG), but not for less oriented ZYH-grade HOPG, indicated a link between the orientational order dependence of the HOPG response above and below the phase transformation stress. To gain insight into this link and into the mechanical response of HOPG shocked to peak stresses approaching the phase transformation onset, the compressibility of ZYB- and ZYH-grade HOPG in the shocked state was examined using front surface impact experiments. Particle velocity histories and sound velocities were measured for peak stresses reaching 18 GPa. Although the locus of the measured peak stress-particle velocity states is indistinguishable for the two grades of HOPG, the measured sound velocities in the peak state reveal significant differences between the two grades. Specifically, 1) The measured sound velocities are somewhat higher for ZYH-grade HOPG, compared to ZYB-grade HOPG. 2) The measured sound velocities for ZYH-grade HOPG increase smoothly with compression, whereas those for ZYB-

grade HOPG exhibit a significant reduction in the compression dependence from 12 GPa to 17 GPa and an abrupt increase from 17 GPa to 18 GPa. 3) The longitudinal moduli, determined from the measured sound velocities, are smaller than the calculated bulk moduli for ZYB-grade HOPG shocked to peak stresses above 15 GPa, indicating the onset of an elastic instability. The present findings demonstrate that the softening of the longitudinal modulus (or elastic instability) presented here is linked to the large elastic waves and the rapid phase transformation reported previously – all observed only for shocked ZYB-grade HOPG. The elastic instability in shocked ZYB-grade HOPG is likely a precursor to the rapid phase transformation observed above 18 GPa for this HOPG grade.

19 April 2024 13:09:15

I. INTRODUCTION

In the early 1990s, Erskine and Nellis reported time-resolved particle velocity measurements on highly oriented pyrolytic graphite (HOPG) samples shock-compressed to 27-50 GPa peak stresses.[1,2] Their measurements revealed significant differences in the shock wave response of two HOPG grades that differed in their orientational order. Wave profiles for the more highly oriented ZYB-grade HOPG exhibited clean two-wave structures, indicating a rapid phase transformation with reported onset stresses as low as 18.6 GPa. In contrast, the lone wave profile reported for the less oriented ZYH-grade HOPG exhibited only a single wave and significant particle velocity fluctuations in the peak state. These results showed that the response of HOPG shocked to stresses above 18 GPa, including the onset of a rapid phase transformation, depends strongly on the HOPG orientational order. However, this strong orientational order dependence was not well understood, in part, due to the lack of corresponding time-resolved measurements on HOPG shocked below 18 GPa.

Subsequently, time-resolved particle velocity measurements for ZYB- and ZYH-grade HOPG shock-compressed to stresses below 18 GPa revealed significant differences in their mechanical response.[3] Measured wave profiles for shocked ZYB-grade HOPG revealed two-wave structures (elastic-inelastic response) having large elastic wave amplitudes; the elastic wave amplitudes increased with increasing peak stress, reaching 16 GPa for a peak stress of 18 GPa. In contrast, wave profiles for shocked ZYH-grade HOPG exhibited single overdriven waves, indicating a negligible elastic wave amplitude. These results showed that the elastic-inelastic response of

19 April 2024 13:09:15

HOPG shocked below 18 GPa also depends strongly on the HOPG orientational order. Because ZYB-grade HOPG was the only pyrolytic graphite that displayed large elastic compression below 18 GPa and a rapid phase transformation above 18 GPa, these results demonstrated a link between the orientational order dependence of the HOPG shock response for peak stresses below and above 18 GPa. Based on this link, the following physical picture was suggested for the rapid phase transformation onset in shocked ZYB-grade HOPG:[3] due to the large elastic compression, the strain energy accumulated in shocked ZYB-grade HOPG leads to an elastic instability that initiates the rapid (displacive) phase transformation.

Despite the strong orientation dependence observed in the previous wave profile measurements for ZYB- and ZYH-grade HOPG shocked below 18 GPa, the locus of peak stress-density compression states determined for the two HOPG grades was indistinguishable within experimental precision.[3] This finding, together with the physical picture proposed previously[3] for the rapid phase transformation onset in shocked ZYB-grade HOPG, raises the following questions: (1) Does the orientational order have a discernable effect on the peak state of shocked HOPG? (2) If so, is there a link between the orientational order dependence of the peak state of HOPG shocked below 18 GPa and the rapid phase transformation in ZYB-grade HOPG shocked above 18 GPa? (3) Does the peak state of ZYB-grade HOPG shocked to stresses approaching 18 GPa show evidence of an elastic instability?

In a recent study on shocked aluminum single crystals,[4] peak stress-density states and sound velocities in the peak states were measured in crystals shocked along different orientations. The results showed that the sound velocity measurements, a

19 April 2024 13:09:15

measure of the longitudinal compressibility in the shocked state, provided better insight into the mechanical state of the shocked Al single crystals than the stress-density results.

Therefore, to address the above stated questions regarding the response of HOPG shocked to stresses below 18 GPa, we examined the peak state compressibility of both HOPG grades using front surface impact experiments. Particle velocity histories were measured at the sample impact surface to determine the stress-particle velocity states, the sound velocities, and the longitudinal elastic moduli in the peak state for both HOPG grades shocked to stresses ranging from 9-18 GPa.

The remainder of the paper is organized as follows: The experimental methods are summarized in Sec. II and the measured wave profiles are presented in Sec. III. In Sec. IV, an analysis of the measured data is presented, together with calculated results from numerical simulations and a discussion of the results. A summary of the main findings and the overall conclusions of this study are presented in Sec. V.

19 April 2024 13:09:15

II. EXPERIMENTAL METHODS

A. Sample characterization

The ZYH- and ZYB-grade HOPG samples (Momentive, Columbus, OH) used in this study were the same two HOPG grades that were examined in previous shock wave transmission experiments.[1-3] Because details regarding the HOPG samples were published previously,[3] only a brief summary is presented here. Although the HOPG samples were not single crystals, the average normal to the sample surface was along the *c*-axis (normal to the basal planes). The manufacturer's specification for the mosaic

spread, which characterizes the orientational order of pyrolytic graphite, was 3.5°±1.5° for the less ordered ZYH-grade HOPG, and 0.8°±0.2° for the more ordered ZYB-grade HOPG. The initial density of each sample used in the shock experiments was measured using the Archimedean method and the results are listed in Table 1. The average initial sample density for both HOPG grades was 2.26 ± 0.01 g/cc, which is comparable to the single crystal density. As discussed previously,[3] attempts to determine ambient longitudinal and shear sound velocities for these two grades of HOPG did not produce reliable results due to the considerable attenuation and distortion of the measured acoustic waves.

B. Front surface impact experiments

Plate impact experiments were performed using the front surface impact configuration shown schematically in Fig. 1. Using a powder gun, an impactor consisting of an HOPG sample, backed by a thick polymethyl methacrylate (PMMA) plate, was launched against a [100] lithium fluoride (LiF) window. Upon impact, shock waves propagated in the HOPG sample and the LiF window. The HOPG sample was oriented such that the shock wave compression was along the average *c* axis. Both sides of the HOPG sample were freshly cleaved prior to the impactor assembly. Experimental parameters for each experiment are listed in Table I.

For the range of peak stresses examined here, shock waves propagated as single overdriven waves in the ZYH-grade HOPG,[3] reaching State A in Fig. 2; and as distinct elastic and inelastic waves (two-wave profile) in the ZYB-grade HOPG,[3] reaching States A and B in Fig. 3. When the shock wave (elastic wave for the ZYB-

19 April 2024 13:09:15

grade HOPG) reaches the back of the HOPG sample, it reflects from the PMMA-HOPG interface as a release wave and unloads the peak stress in the HOPG. Because the leading edge of a release wave travels at the longitudinal sound speed in the shocked material,[4,5] its arrival at the impact surface enables a determination of the sound velocity in the shocked HOPG. Further details are provided in Sec. IV.

To determine the peak state in the HOPG sample and the release wave arrival time at the impact surface, the particle velocity history at the center of the LiF window was measured using a velocity interferometer system (VISAR)[6] operating at a laser wavelength of 532 nm (Fig. 1). A gold film was vapor-deposited on the impact surface of the LiF window to reflect the laser light. To minimize the loss of reflected light upon impact, the impact surface of the LiF window was roughened (by lapping) prior to the deposition of the gold film.[7] In all the experiments, particle velocity histories were measured using a dual velocity-per-fringe configuration to minimize uncertainties in the peak particle velocity. The measured apparent velocities were corrected for the presence of the LiF window using the procedure reported by Wise and Chhabildas.[8] Four piezoelectric (PZT) pins (Dynasen Inc., Goleta, CA) were mounted concentrically on the back of the LiF window, as shown in Fig. 1, to determine the impact (and shock wave) tilt. This information is used to accurately determine the wave velocities.[3]

19 April 2024 13:09:15

III. RESULTS

A total of 15 front surface impact experiments were conducted on ZYH- and ZYB-grade HOPG samples. The impact velocities for these experiments were chosen so that the peak stresses in the HOPG samples corresponded to those reached in the previous

wave transmission experiments (9-18 GPa).[3] Thus, the peak stresses were less than the lowest phase transformation stress reported for shocked HOPG (18.6 GPa).[2]

Particle velocity profiles for each experiment, measured at the HOPG sample-LiF window interface (impact surface), are shown in Figs. 4 and 5. Figure 4 shows the measured profiles for shocked ZYH-grade HOPG (experiments 1-7). All the profiles exhibit an initial jump upon impact, followed by a constant (peak) state, and, subsequently, a featureless decrease from the peak particle velocity, marking the arrival of the release wave from the back of the impactor (see Fig. 2). Comparison of the results from experiments 3 and 4, which had similar impact velocities, demonstrates good experimental reproducibility. The measured peak particle velocities for the profiles in Fig. 4 are shown in Table II.

Figure 5 shows the measured wave profiles for shocked ZYB-grade HOPG (experiments 8-15). Similar to the results for ZYH-grade HOPG (Fig. 4), all the profiles in Fig. 5 exhibit an initial jump in particle velocity at impact, followed by a constant (peak) state, and, subsequently, the arrival of a featureless release wave (see Fig. 3). Good experimental reproducibility for shocked ZYB-grade HOPG is demonstrated by comparing the results from experiments 14 and 15, which had similar impact velocities. The measured peak particle velocities for the profiles in Fig. 5 are shown in Table II.

In Figs. 4 and 5, many of the measured wave profiles exhibit sharp dips that occur in the peak state and/or at the trailing edge of the unloading wave. Although the cause of the dips is not known with certainty, those appearing in the peak state are likely due to the interaction of the shock wave with small delaminations in the interior of the HOPG samples. Similarly, the dips at the trailing edge of the unloading wave likely

19 April 2024 13:09:15

result from debonding, prior to impact, of the HOPG sample from the PMMA backing plate. In our analysis of the measured wave profiles, presented next, no correlation was found between the presence (or absence) of the dips and the detailed features of the analyzed results. Therefore, the dips are ignored in all subsequent discussion.

IV. ANALYSIS AND DISCUSSION

The experimentally measured wave profiles in Figs. 4 and 5 were analyzed to provide the peak or shocked states, the sound velocities, and the longitudinal moduli in the shocked states.

A. Peak states

Because of the continuity of longitudinal stresses and particle velocities across the HOPG-LiF interface (impact surface), particle velocity histories at the impact surface and published LiF Hugoniot data[9] provide a direct determination of the peak stresses attained in the shocked HOPG samples. The Hugoniot relationship used here for LiF is $U_s = 5.148 + 1.353u_p$,[9] where U_s and u_p are the shock velocity and particle velocity, respectively. From the measured peak stress, the density compression in the peak state was determined using the peak stress-compression curve for shocked HOPG obtained previously from wave transmission experiments.[3] The peak longitudinal stresses and peak density compressions determined here for shocked HOPG are shown in Table II.

In Fig. 6, the measured peak stress-particle velocity states for shocked ZYH- and ZYB-grade HOPG (solid symbols) from the present work are shown, together with the peak states determined from the previous wave transmission experiments (open

19 April 2024 13:09:15

symbols).[3] Within experimental precision (1-2%), the locus of measured peak states for shocked ZYH-grade HOPG is the same as that for shocked ZYB-grade HOPG. In addition, the peak states for shocked ZYH- and ZYB-grade HOPG measured in the front surface impact experiments are well matched to the peak states obtained in the previous wave transmission experiments.[3] This good agreement demonstrates the consistency between the two sets of experiments.

B. Sound velocities

For both grades of HOPG, the Lagrangian sound velocity in shocked HOPG in the peak state was determined from the measured arrival time of the release wave at the sample-window interface. For ZYH-grade HOPG (experiments 1-7), a single overdriven shock wave propagates in the HOPG samples.[3] Therefore, the Lagrangian sound velocity c_L in the peak state was determined using the following expression for the measured arrival time t_2 of the release wave (see Fig. 2):

$$t_2 = \frac{h_s}{U_s} + \frac{h_s}{c_L}, \tag{1}$$

where h_s is the initial sample thickness (taking into account corrections for the effect of impact tilt), and U_s is the velocity of the overdriven wave, determined from the measured peak particle velocity and peak stress using the Rankine-Hugoniot jump conditions.[10] The release wave arrival time t_2 was determined from the intersection of two straight lines that were fit to the measured wave profiles: one line was fit to the peak state particle velocity and the other was fit to the early portions of the unloading wave.

For ZYB-grade HOPG (experiments 8-15), a two-wave structure (elastic and inelastic waves) arises in the HOPG samples.[3] Therefore, the Lagrangian sound

19 April 2024 13:09:15

velocity c_L in the peak state was determined using the following expression for the arrival time t_2 of the release wave, which corresponds to the wave propagation details shown in Fig. 3:

$$t_2 = \frac{h_s}{U_{sA}} + \frac{h_1}{U_{RA}} + \frac{(h_s - h_1)}{c_L}. \quad (2)$$

In equation (2), h_s is the initial sample thickness (taking into account corrections for the effect of impact tilt), and h_1 is the Lagrangian position in the HOPG sample where the reflected elastic release wave (from the HOPG/PMMA interface) interacts with the oncoming inelastic wave (see Fig. 3a). The velocity of the elastic wave (U_{sA}) was determined from the measured peak stress using the elastic wave amplitude (σ_{xA}) – peak stress (σ_{xB}) relationship determined previously for ZYB-grade HOPG (see Fig. 8 from Ref. 3),

$$\sigma_{xA} = 1.26 + 0.81\sigma_{xB}, \quad (3)$$

together with the elastic Hugoniot curve for ZYB-grade HOPG[3] and the Rankine-Hugoniot jump conditions.[10] The Lagrangian elastic release wave velocity (U_{RA}) was determined by assuming that ZYB-grade HOPG released from the elastically-compressed state (State A in Fig. 3) along the elastic Hugoniot curve. The position h_1 was determined by solving the equation (see Fig. 3a):

$$\frac{h_s}{U_{sA}} + \frac{h_1}{U_{RA}} = \frac{(h_s - h_1)}{U_{sB}}, \quad (4)$$

where the Lagrangian inelastic wave velocity U_{sB} was determined from the stress and density compression in the elastically-compressed state (A) and in the peak state (B) using the Rankine-Hugoniot jump conditions.[10] The release wave arrival time t_2 was

19 April 2024 13:09:15

determined from the intersection of two straight lines that were fit to the measured wave profiles using the same approach as that used for ZYH-grade HOPG.

Table II lists the Lagrangian sound velocities c_L determined for ZYH- and ZYB-grade HOPG in the shocked state. The uncertainties shown in Table II were determined from the individual sources, including initial sample thickness and density, impact velocity, peak particle velocity, and arrival time of the release wave. The uncertainties from the different sources were combined using standard methods of uncertainty propagation.[11]

Compression-corrected (or Eulerian) sound velocities account for changes in sample thickness due to shock wave compression and correspond to the material stiffness in the peak state. For shocked ZYH- and ZYB-grade HOPG, the Eulerian sound velocities were obtained by dividing the Lagrangian sound velocities by the density change (ρ / ρ_0) and are listed in Table II.

Figure 7 shows the Eulerian sound velocities as a function of density compression and longitudinal stress (solid symbols). These results show that the measured sound velocities for shocked ZYH-grade HOPG are somewhat larger than those for shocked ZYB-grade HOPG. More importantly, the compression dependence of the sound velocity for shocked ZYH-grade HOPG differs significantly from that for ZYB-grade HOPG. For ZYH-grade HOPG, the sound velocities increase smoothly over the 10-18 GPa stress range. In contrast, for shocked ZYB-grade HOPG, the sound velocity increases rapidly between 9 GPa and 12 GPa. However, between 12 GPa and 15 GPa, the sound velocity increases slowly, reaching a constant value (within

19 April 2024 13:09:15

experimental precision) between 15 GPa and 17 GPa, before increasing abruptly between 17 GPa and 18 GPa.

C. Numerical simulations

In our previous wave transmission experiments on shocked ZYH- and ZYB-grade HOPG,[3] the measured wave profiles were analyzed using two approaches: an idealized approach to determine the shocked states and the use of numerical simulations. For the numerical simulations, phenomenological material models were developed for shocked ZYH- and ZYB-grade HOPG that provided good agreement between the calculated and the measured wave profiles for both HOPG grades.[3] To supplement the idealized analysis presented in Sec. IV.B, and to provide an important link to our previous results,[3] we carried out numerical simulations of the present front surface impact experiments using the same phenomenological material models used previously. A brief summary of the material models and the simulation methods is provided in the Appendix.

The calculated wave profiles (not shown) for shocked ZYH- and ZYB-grade HOPG provide a good overall match to the measured profiles shown in Figs. 4 and 5, including the featureless release waves. The calculated results indicate a complete loss of strength (zero stress deviators in the peak state) for both HOPG grades, in agreement with our previous calculations.[3] The calculated particle velocities, stresses, and density compressions in the peak state, presented in Table II, are in good agreement with those determined from the measured wave profiles. The good agreement between the calculated and the measured results for the front surface

19 April 2024 13:09:15

impact experiments presented here, together with that for the previous wave transmission experiments,[3] demonstrates that the material models provide a reliable phenomenological description of the response of ZYH- and ZYB-grade HOPG shocked to stresses reaching 18 GPa.

Calculated sound velocities for shocked ZYH- and ZYB-grade HOPG were determined from the numerical simulations by tracking the propagation of the simulated release wave through the shocked sample (see Figs. 2 and 3). Because the calculations indicate complete loss of strength in the peak state for both HOPG grades, the calculated sound velocities correspond to the mean stress (or bulk) response. The calculated Lagrangian sound velocities, together with the corresponding Eulerian sound velocities are presented in Table II. Because the same mean stress-density curve was incorporated in the material models for both HOPG grades, the calculated bulk sound velocities for the two HOPG grades were fitted well by a single curve, shown by the dashed line in Fig. 7. As shown in the figure, the calculated bulk sound velocity increases smoothly with increasing density compression (or stress).

To determine sound velocities that correspond to the calculated longitudinal response, the material models for ZYH- and ZYB-grade HOPG were modified slightly so that small, but non-zero, stress deviators were obtained in the calculated peak state (see Appendix). Because the same mean stress-density curve and the same shear modulus were used in the material models for both HOPG grades, the calculated longitudinal sound velocities for the two HOPG grades were again fitted well by a single curve, shown as the solid line in Fig. 7. The calculated longitudinal sound velocity increases smoothly with increasing density compression (or stress), similar to the

19 April 2024 13:09:15

calculated bulk values. The calculated longitudinal and bulk sound velocities are compared next with the measured results.

D. Discussion

The direct measurements of peak stress and peak particle velocity presented here (Fig. 6) show that, within experimental uncertainties, the peak stress-particle velocity states for the two HOPG grades are indistinguishable, consistent with previous results from the transmission experiments.[3] In contrast, the measured sound velocities (Figs. 7) reveal significant differences in the peak state compressibility for ZYH- and ZYB-grade HOPG, showing that the peak state of HOPG shocked below 18 GPa depends strongly on the HOPG orientational order. The sound velocity (or compressibility) results are a better indicator of the mechanical state of shocked ZYH- and ZYB-grade HOPG, compared to stress-particle velocity or stress-compression results.

For ZYH-grade HOPG, the measured sound velocities in Fig. 7 are intermediate between the calculated longitudinal and bulk velocities; the measured velocities increase smoothly with compression, similar to the calculated velocities. For ZYB-grade HOPG beyond 12 GPa, the measured sound velocities do not increase smoothly with compression. Instead, a number of interesting features are observed with increasing compression: beyond ~18 percent compression, the measured sound speed is first nearly identical to the bulk sound speed and then drops below the bulk sound speed; around 21 percent compression, the measured sound speed increases and reaches the bulk sound speed at the highest compression (~22 percent).

19 April 2024 13:09:15

Longitudinal moduli for shocked ZYH- and ZYB-grade HOPG were determined from the measured Eulerian sound velocities and peak densities and are listed in Table II. For comparison, longitudinal and bulk moduli were also determined from the calculated sound velocities. Figure 8 shows the measured longitudinal moduli (solid symbols) and the calculated longitudinal and bulk moduli (solid and dashed lines, respectively) as a function of density compression and longitudinal stress. As shown in Fig. 8, the compression-dependence of the measured longitudinal modulus for shocked ZYB-grade HOPG is significantly reduced between 12 and 18 GPa, indicating a softening of the longitudinal modulus.

To better understand the observed softening, we examined the shear modulus G for shocked HOPG,[10]

$$G = \frac{3}{4}(L - B), \tag{5}$$

where L and B are the measured longitudinal modulus and the calculated bulk modulus, respectively. Although equation (5) is strictly applicable only for isotropic solids, its use here is consistent with the material description for shocked HOPG presented in the Appendix and in Ref. 3. Because the measured longitudinal modulus for shocked ZYB-grade HOPG is less than the calculated bulk modulus for peak stresses between 15 GPa and 18 GPa (see Fig. 8), the shear modulus from equation (5) is negative over the same range of peak stresses. A negative shear modulus violates the well-known criteria for elastic stability,[12,13] and the measured results in Fig. 8 show that an elastic instability occurs in ZYB-grade HOPG shocked to peak stresses between 15 GPa and 18 GPa.

The strong orientational order dependence of the shocked state, shown in Figs. 7 and 8, is consistent with other types of orientation dependence reported previously [1-3]

19 April 2024 13:09:15

for HOPG shocked to stresses below and above 18 GPa. We list these linkages: the softening of the longitudinal modulus for ZYB-grade HOPG shocked between 12 and 18 GPa (Fig. 8), the large amplitude elastic waves observed for ZYB-grade HOPG shocked below 18 GPa,[3] and the rapid phase transformation for ZYB-grade HOPG shocked above 18 GPa.[1,2] The present results and the large elastic wave amplitudes reported previously[3] suggest that the longitudinal modulus softening, and the associated elastic instability, in ZYB-grade HOPG may be the result of large elastic compressions. Because the elastic instability occurs at stresses well below the onset of rapid phase transformation,[1-2] the elastic instability is likely a precursor to the rapid phase transformation in shocked ZYB-grade HOPG.

The findings presented here are consistent with the following physical picture proposed for the onset of a rapid phase transformation in shocked ZYB-grade HOPG:[3] the large strain energy in the compressed state is a consequence of the large elastic compression and results in an elastic instability, which leads to the onset of a displacive phase transformation. Real-time, in situ, microscopic measurements[14,15] are needed to provide direct confirmation of this picture.

19 April 2024 13:09:15

V. SUMMARY AND CONCLUSIONS

To gain insight into the orientational order dependence of shocked HOPG observed[1-3] at stresses below and above the phase transformation onset (18.6 GPa), we examined the compressibility of shocked ZYH- and ZYB- grade HOPG at stresses approaching 18 GPa. Particle velocity histories were measured in front surface impact experiments for peak stresses between 9 and 18 GPa. The results showed that, within

experimental precision, the locus of measured peak stress-particle velocity states for ZYH- and ZYB-grade HOPG is indistinguishable. In contrast, the measured sound velocities and the corresponding longitudinal moduli in the peak state revealed key differences between ZYH- and ZYB-grade HOPG:

1. For the ZYH-grade, the sound velocities increase smoothly over the range of peak stresses examined here. In contrast, the compression-dependence of the sound velocities for ZYB-grade HOPG exhibits a significant reduction between 12 and 17 GPa, indicating an increase in compressibility (or softening of the longitudinal modulus), and an abrupt increase in sound velocity between 17 and 18 GPa.
2. For ZYH-grade HOPG, the longitudinal moduli determined from the measured sound velocities are larger than the calculated bulk moduli over the range of peak stresses examined here. In contrast, the longitudinal moduli for ZYB-grade HOPG are smaller than the calculated bulk moduli for stresses between 15 and 18 GPa, implying the onset of an elastic instability.

These findings show that sound velocity measurements are a better indicator of differences in the peak state of shocked ZYH- and ZYB-grade HOPG than stress-particle velocity (Fig. 6) or stress-density compression[3] measurements. The measured sound velocities (Fig. 7) and the corresponding longitudinal moduli (Fig. 8) for the two grades of HOPG depend strongly on the HOPG orientational order for peak stresses below the phase transition onset.

19 April 2024 13:09:15

Our findings establish a link between the following phenomena, observed only for shocked ZYB-grade HOPG: softening of the longitudinal modulus for peak stresses below 18 GPa (Fig. 8), large amplitude elastic waves for stresses below 18 GPa,[3] and rapid phase transformation for stresses above 18 GPa.[1,2] The large amplitude elastic waves observed previously[3] and the observed longitudinal modulus softening (elastic instability) for shocked ZYB-grade HOPG suggest that the elastic instability is likely a consequence of the large elastic compression for this HOPG grade. Furthermore, the elastic instability below the phase transition stress and the rapid phase transformation reported for stresses above 18.6 GPa[1,2] suggest that the elastic instability is likely a precursor to the phase transformation in shocked ZYB-grade HOPG.

Overall, the present findings are consistent with the physical picture suggested previously[3] for the rapid phase transformation in shocked ZYB-grade HOPG: Large elastic compressions result in an elastic instability, which leads to the onset of a displacive phase transformation. However, microscopic measurements[14,15] are needed to confirm this hypothesis and to gain further insight into the peak state structure of shocked ZYB-grade HOPG.

19 April 2024 13:09:15

ACKNOWLEDGMENTS

Nate Arganbright, Paul Ruggiero, Brendan Williams and Kurt Zimmerman are thanked for their expert assistance with the experiments. This work was supported by the Department of Energy/NNSA through Cooperative Agreement DE-NA0000970.

APPENDIX: NUMERICAL SIMULATIONS

The phenomenological material models used in the numerical simulations presented in Sec. IV.C are the same as those used previously to simulate transmitted wave profiles in shocked ZYH- and ZYB-grade HOPG.[3] Summarized briefly, our modeling approach incorporated the usual separation[16] of the mechanical response into the mean stress response and the deviatoric stress response. The mean stress curves for ZYH- and ZYB-grade HOPG were assumed to be identical and were fit to the combined peak stress-density compression data for the two HOPG grades.[3] For ZYH-grade HOPG, which exhibited single or overdriven wave profiles,[3] the stress deviators were assumed to be zero. For ZYB-grade HOPG, which exhibited two-wave elastic-inelastic profiles,[3] the stress deviators were determined using a time-dependent overstress model,[17] in which the shear modulus and yield stress depend on longitudinal stress, and the yield stress decreases with accumulated inelastic strain (loss of strength).[3]

For some of the calculations presented in Sec. IV.C, the models for ZYH- and ZYB-grade HOPG were modified slightly so that a small, but non-zero, yield stress was retained in the calculated peak states. For the modified ZYH-grade HOPG model, the shear modulus was assumed to be the same as that used for ZYB-grade HOPG.

The numerical simulations were carried out using a one-dimensional wave propagation code,[18] which utilizes the typical finite-difference, artificial viscosity approach[16] to solve the governing equations for large amplitude wave propagation. The responses of the [100] LiF window and the PMMA backing plate on the impactor were described using fits to published shock wave data.[9,19,20]

19 April 2024 13:09:15

REFERENCES

[1] D. J. Erskine and W. J. Nellis, Nature **349**, 317 (1991).

[2] D. J. Erskine and W. J. Nellis, J. Appl. Phys. **71**, 4882 (1992).

[3] M. Lucas, J. M. Winey, and Y. M. Gupta, J. Appl. Phys. **114**, 093515 (2013).

[4] D. Choudhuri and Y. M. Gupta, J. Appl. Phys. **114**, 153504 (2013).

[5] B. J. Jensen, F. J. Cherne, J. C. Cooley, M. V. Zhernokletov, and A. E. Kovalev, Phys. Rev. B **81**, 214109 (2010).

[6] L. M. Barker and R. E. Hollenbach, J. Appl. Phys. **43**, 4669 (1972).

[7] J. R. Asay and L. M. Barker, J. Appl. Phys. **45**, 2540 (1974).

[8] J. L. Wise and L. C. Chhabildas, in *Shock Waves in Condensed Matter – 1985*, edited by Y. M. Gupta (Plenum, New York, 1986), p. 441.

[9] W. J. Carter, High Temp. - High Press. **5**, 313 (1973).

[10] R. G. McQueen, S. P. Marsh, and J. N. Fritz, J. Geophys. Res. **72**, 4999 (1967).

[11] J. R. Taylor, *An Introduction to Error Analysis* (University Science Books, Mill Valley, CA, 1982).

[12] M. Born and K. Huang, *Dynamical Theory of Crystal Lattices* (Oxford University Press, Oxford, 1962), p. 144.

[13] R. Hill and F. Milstein, Phys. Rev. B **15**, 3087 (1977).

[14] S. J. Turneaure and Y. M. Gupta, J. Appl. Phys. **105**, 053520 (2009).

[15] S. J. Turneaure and Y. M. Gupta, J. Appl. Phys. **106**, 033513 (2009).

[16] M. L. Wilkins, in *Methods in Computational Physics*, edited by B. Alder, S. Fernbach, and M. Rotenberg (Academic, New York, 1964), Vol. 3, p. 211.

19 April 2024 13:09:15

[17] G. Yuan, R. Feng, Y. M. Gupta, and K. Zimmerman, J. Appl. Phys. **88**, 2371 (2000).

[18] Y. M. Gupta, COPS Wave Propagation Code (SRI International, Menlo Park, CA, 1976).

[19] L. M. Barker and R. E. Hollenbach, J. Appl. Phys. **41**, 4208 (1970).

[20] K. W. Schuler and J. W. Nunziato, Rheol. Acta **13**, 265 (1974).

19 April 2024 13:09:15

Table I. Summary of experimental parameters.

Experiment number	Sample	Sample density[a] (g/cc)	Sample thickness[b] (mm)	Impact velocity[c] (mm/μs)
1 (13-617)	ZYH HOPG	2.26	0.930	1.439
2 (13-627)	ZYH HOPG	2.25	0.970	1.678
3 (14-611)	ZYH HOPG	2.25	0.939	1.820
4 (14-607)	ZYH HOPG	2.26	0.998	1.827
5 (13-613)	ZYH HOPG	2.26	0.970	2.000
6 (13-616)	ZYH HOPG	2.26	0.894	2.206
7 (13-619)	ZYH HOPG	2.26	0.884	2.261
8 (13-611)	ZYB HOPG	2.26	0.975	1.250
9 (13-628)	ZYB HOPG	2.25	0.897	1.595
10 (14-605)	ZYB HOPG	2.26	1.001	1.784
11 (13-608)	ZYB HOPG	2.27	0.856	1.965
12 (13-626)	ZYB HOPG	2.25	1.024	2.086
13 (13-609)	ZYB HOPG	2.26	0.912	2.167
14 (13-621)	ZYB HOPG	2.25	0.996	2.297
15 (13-620)	ZYB HOPG	2.27	0.947	2.293

[a] Measurement uncertainties are 0.2% or better.
[b] Measurement uncertainties are 0.3% or better.
[c] Measurement uncertainties are 0.5% or better.

19 April 2024 13:09:15

Table II. Experimental results for shocked highly-oriented pyrolytic graphite.[a]

Experiment number	Sample	Particle velocity[b] (mm/μs)	Peak stress (GPa)	Density compression $\mu=\rho/\rho_O-1$	Lagrangian sound velocity (mm/μs)	Eulerian sound velocity (mm/μs)	Longitudinal modulus[c] (GPa)
1 (13-617)	ZYH HOPG	0.649±0.008	10.33±0.14	0.156±0.001	8.97±0.28	7.76±0.25	157±10
		(0.651)	(10.36)	(0.157)	(8.01)	(6.93)	(125)
2 (13-627)	ZYH HOPG	0.768±0.006	12.54±0.11	0.175±0.001	9.27±0.18	7.89±0.16	165±7
		(0.768)	(12.54)	(0.176)	(8.73)	(7.42)	(146)
3 (14-611)	ZYH HOPG	0.840±0.007	13.94±0.13	0.186±0.001	9.60±0.21	8.10±0.18	175±8
		(0.838)	(13.90)	(0.186)	(9.11)	(7.69)	(158)
4 (14-607)	ZYH HOPG	0.851±0.007	14.15±0.14	0.187±0.001	9.63±0.19	8.11±0.17	177±7
		(0.841)	(13.96)	(0.187)	(9.12)	(7.68)	(158)
5 (13-613)	ZYH HOPG	0.924±0.006	15.61±0.13	0.198±0.001	10.01±0.20	8.35±0.17	189±8
		(0.928)	(15.68)	(0.199)	(9.61)	(8.02)	(174)
6 (13-616)	ZYH HOPG	1.024±0.007	17.66±0.16	0.211±0.001	10.64±0.22	8.78±0.18	211±9
		(1.031)	(17.80)	(0.212)	(10.23)	(8.44)	(195)
7 (13-619)	ZYH HOPG	1.055±0.004	18.31±0.08	0.215±0.001	10.67±0.14	8.78±0.11	212±6
		(1.059)	(18.39)	(0.216)	(10.38)	(8.54)	(200)
8 (13-611)	ZYB HOPG	0.564±0.004	8.80±0.07	0.141±0.001	7.59±0.22	6.65±0.19	114±7
		(0.560)	(8.73)	(0.141)	(7.53)	(6.60)	(112)
9 (13-628)	ZYB HOPG	0.727±0.006	11.76±0.11	0.169±0.001	8.90±0.11	7.61±0.09	152±4
		(0.726)	(11.75)	(0.169)	(8.48)	(7.25)	(139)
10 (14-605)	ZYB HOPG	0.820±0.004	13.55±0.07	0.183±0.001	9.09±0.10	7.68±0.08	158±3
		(0.819)	(13.53)	(0.183)	(9.10)	(7.69)	(158)
11 (13-608)	ZYB HOPG	0.908±0.003	15.28±0.07	0.195±0.001	9.41±0.11	7.87±0.10	168±4
		(0.908)	(15.29)	(0.196)	(9.53)	(7.96)	(171)
12 (13-626)	ZYB HOPG	0.963±0.007	16.41±0.14	0.204±0.001	9.47±0.10	7.87±0.08	168±4
		(0.970)	(16.54)	(0.204)	(9.84)	(8.17)	(182)
13 (13-609)	ZYB HOPG	1.002±0.006	17.20±0.13	0.208±0.001	9.68±0.10	8.01±0.08	175±4
		(1.010)	(17.37)	(0.210)	(10.10)	(8.35)	(191)
14 (13-621)	ZYB HOPG	1.059±0.006	18.40±0.13	0.216±0.001	10.13±0.09	8.33±0.08	190±4
		(1.076)	(18.75)	(0.218)	(10.50)	(8.62)	(205)
15 (13-620)	ZYB HOPG	1.063±0.005	18.48±0.11	0.216±0.001	10.31±0.09	8.47±0.07	198±4
		(1.073)	(18.70)	(0.218)	(10.43)	(8.56)	(202)

[a] The numbers in parentheses are from numerical simulations using the material models presented in Ref. 3.
[b] Indicates the peak particle velocities measured at the impact surface. The uncertainties shown account for the precision of the interferometry measurements and for fluctuations in the measured velocity histories (Figs. 4 and 5).
[c] Calculated moduli (in parentheses) reflect the mean stress (or bulk) response.

19 April 2024 13:09:15

FIGURE CAPTIONS

FIG. 1. Schematic view of the front surface impact experiments to measure particle velocity histories and sound velocities in shocked HOPG.

FIG. 2. (a) Time–position diagram and (b) longitudinal stress–particle velocity diagram for shocked ZYH-grade HOPG. State A is the peak state reached in the HOPG sample by the single overdriven shock wave. In (a), U_s is the velocity of the shock wave in the HOPG sample. The dotted line indicates the release wave due to the reflection of the shock wave from the PMMA-HOPG interface. The leading edge of the release wave propagates at the sound velocity (c_L) in the shocked state and reaches the impact surface at time t_2. In (b), the solid lines are the Hugoniot curves for the HOPG sample and the LiF window.

FIG. 3. (a) Time–position diagram and (b) longitudinal stress–particle velocity diagram for shocked ZYB-grade HOPG. A and B denote the states in the HOPG sample reached by the elastic and inelastic waves, respectively. In (a), U_{sA} and U_{sB} are the velocities of the elastic and inelastic waves in the HOPG sample, respectively. The dotted line indicates the release wave due to the reflection of the elastic wave from the PMMA-HOPG interface. The leading edge of the release wave propagates at a velocity U_{RA} over a distance h_1, until it interacts with the oncoming inelastic wave. The leading edge of the release wave then propagates at the sound velocity (c_L) in the shocked state and

19 April 2024 13:09:15

reaches the impact surface at time t_2. In (b), the solids lines are the Hugoniot curves for the HOPG sample and the LiF window.

FIG. 4. Impact surface particle velocity histories for ZYH-grade HOPG. The experiment numbers correspond to those listed in Tables I and II. Dark red lines correspond to experiments 1, 3, 5 and 7, and light red lines correspond to experiments 2, 4 and 6. The peak stresses range from 10.3 to 18.3 GPa. Time zero corresponds to the moment of impact.

FIG. 5. Impact surface particle velocity histories for ZYB-grade HOPG. The experiment numbers correspond to those listed in Tables I and II. Dark green lines correspond to experiments 8, 10, 12, and 14 and light green lines correspond to experiments 9, 11, 13 and 15. The peak stresses range from 8.8 to 18.5 GPa. Time zero corresponds to the moment of impact.

FIG. 6. Measured peak longitudinal stress – particle velocity states for shocked HOPG. The solid symbols are results from the present experiments. The remaining symbols and curves are from previous wave transmission experiments (Ref. 3). The crossed symbols are the elastic wave states in ZYB-grade HOPG; the open symbols are the peak states in ZYH- and ZYB-grade HOPG. The solid line is a fit to the elastic wave states in the ZYB-grade, and the dashed line is a fit to the combined peak states for both ZYH- and ZYB-grades. The experimental uncertainties for the measured states are small compared to the size of the symbols.

19 April 2024 13:09:15

FIG. 7. Eulerian sound velocity versus density compression and longitudinal stress for shocked HOPG. The solid symbols are measured values. The solid and dashed lines are fits to longitudinal and bulk sound velocities, respectively, calculated using wave propagation simulations.

FIG. 8. Longitudinal modulus versus density compression and longitudinal stress for shocked HOPG. The solid symbols are longitudinal moduli determined from the measured sound velocities. The solid and dashed lines are fits to calculated longitudinal and bulk moduli, respectively, determined from the calculated sound velocities.

19 April 2024 13:09:15

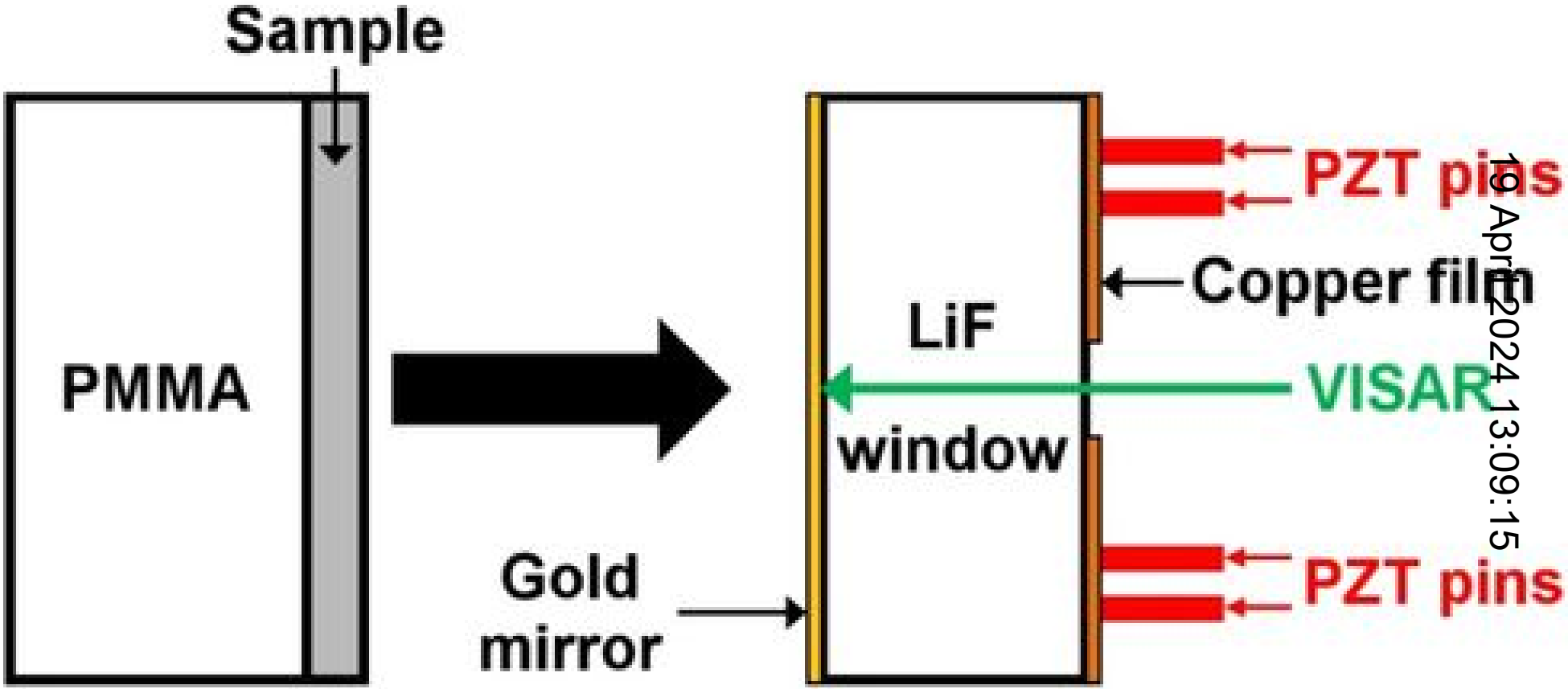

19 April 2024 13:09:15

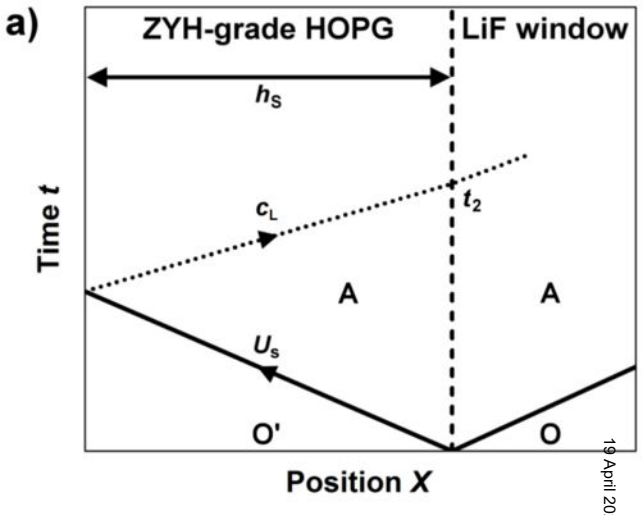

19 April 2024 13:09:15

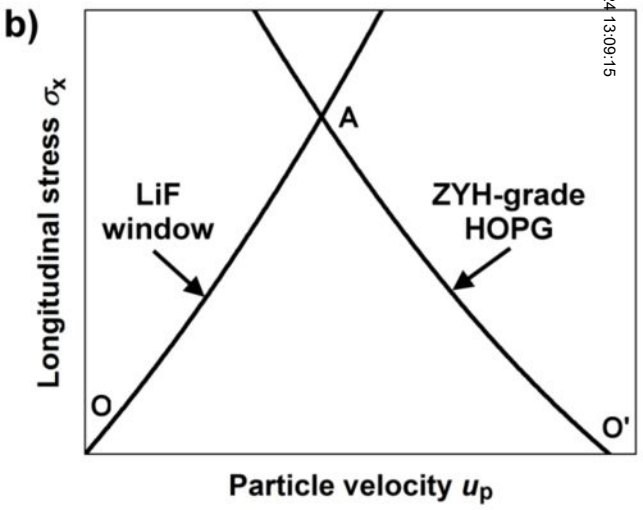

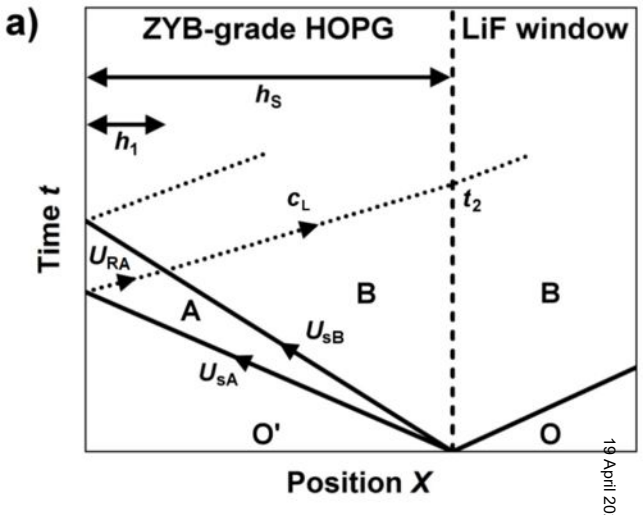

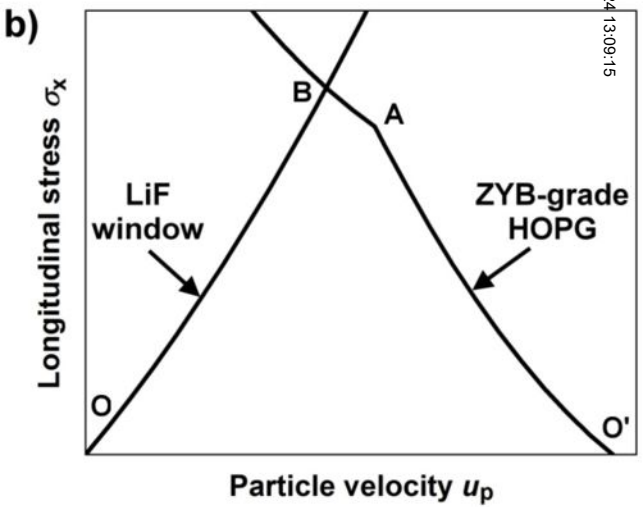

19 April 2024 13:09:15

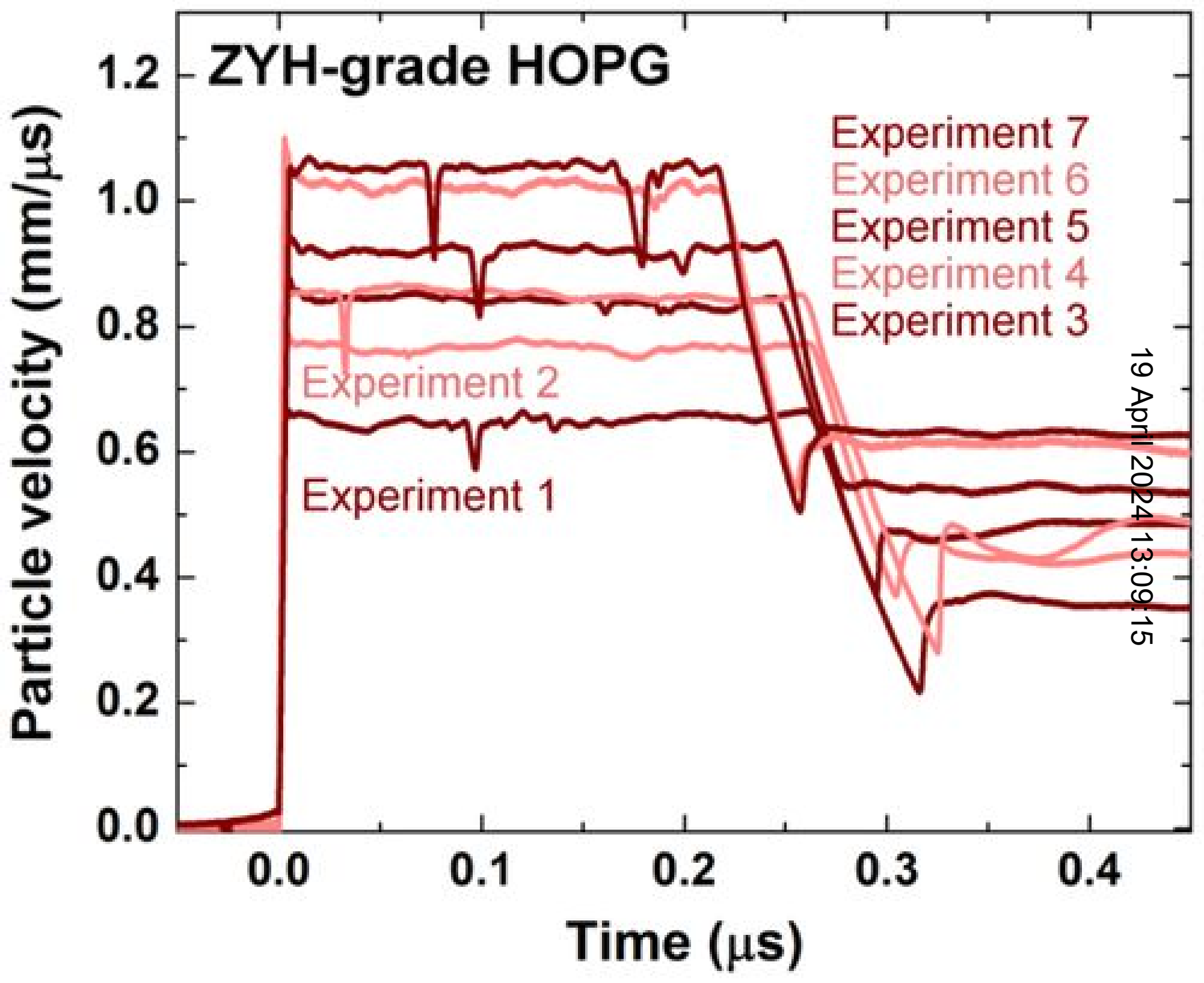
ZYH-grade HOPG
Experiment 7
Experiment 6
Experiment 5
Experiment 4
Experiment 3
Experiment 2
Experiment 1
19 April 2024 13:09:15
Particle velocity (mm/μs)
Time (μs)
0.0
0.2
0.4
0.6
0.8
1.0
1.2
0.0
0.1
0.2
0.3
0.4

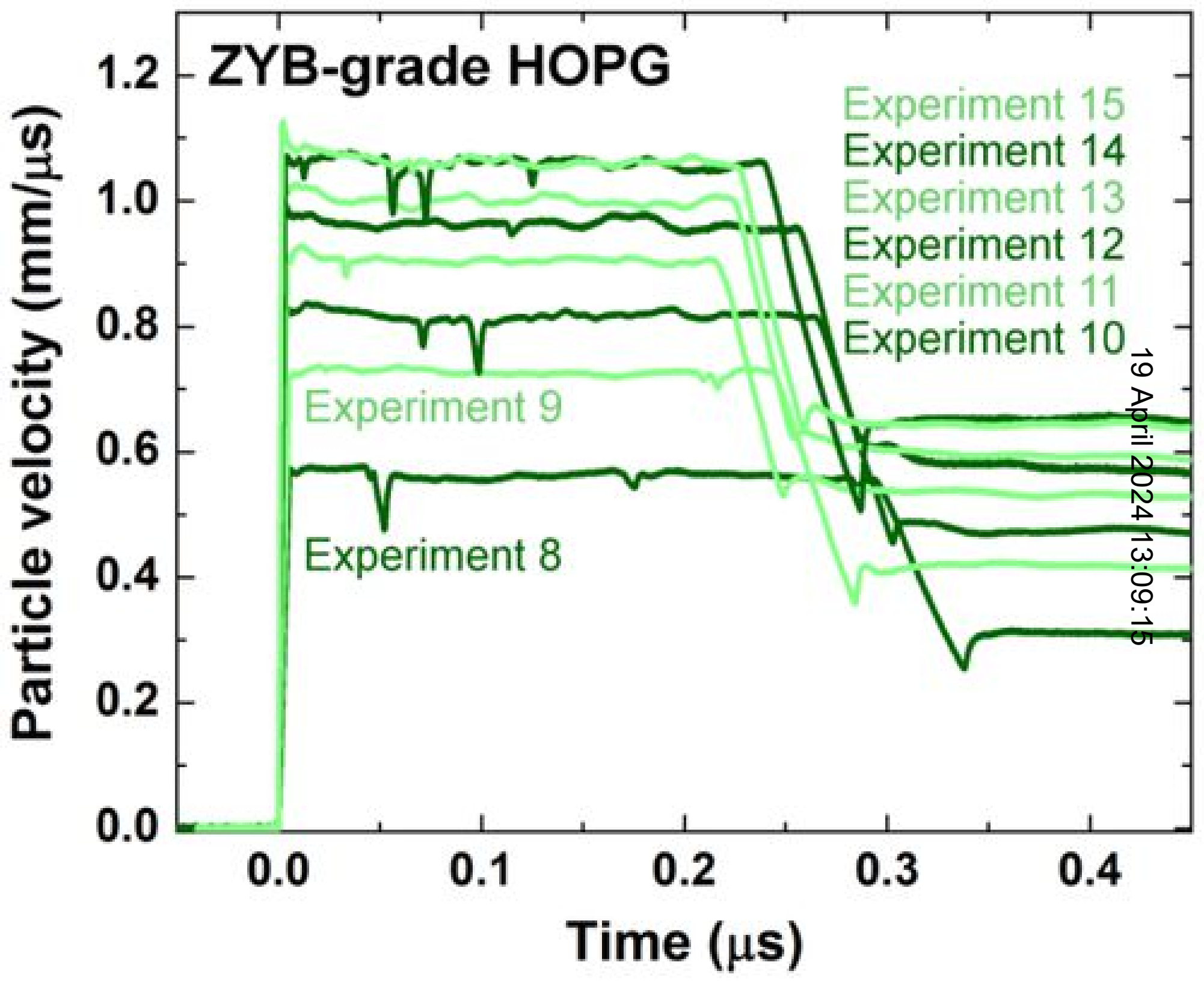
ZYB-grade HOPG
Experiment 15
Experiment 14
Experiment 13
Experiment 12
Experiment 11
Experiment 10
Experiment 9
Experiment 8
19 April 2024 13:09:15
Particle velocity (mm/μs)
Time (μs)
0.0
0.2
0.4
0.6
0.8
1.0
1.2
0.0
0.1
0.2
0.3
0.4

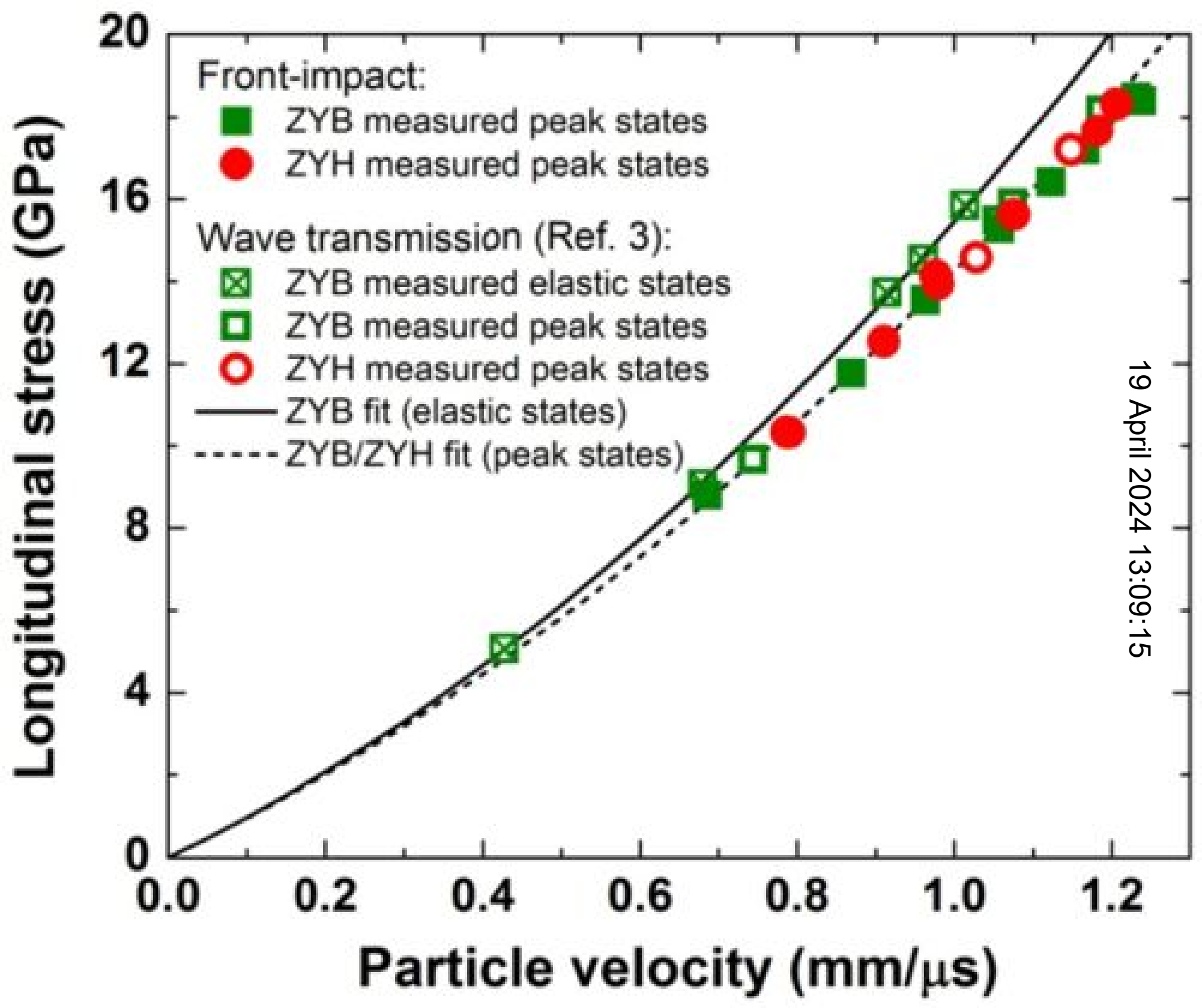
Front-impact:
ZYB measured peak states
ZYH measured peak states
Wave transmission (Ref. 3):
ZYB measured elastic states
ZYB measured peak states
ZYH measured peak states
ZYB fit (elastic states)
ZYB/ZYH fit (peak states)
Longitudinal stress (GPa)
Particle velocity (mm/μs)
0
4
8
12
16
20
0.0
0.2
0.4
0.6
0.8
1.0
1.2
19 April 2024 13:09:15

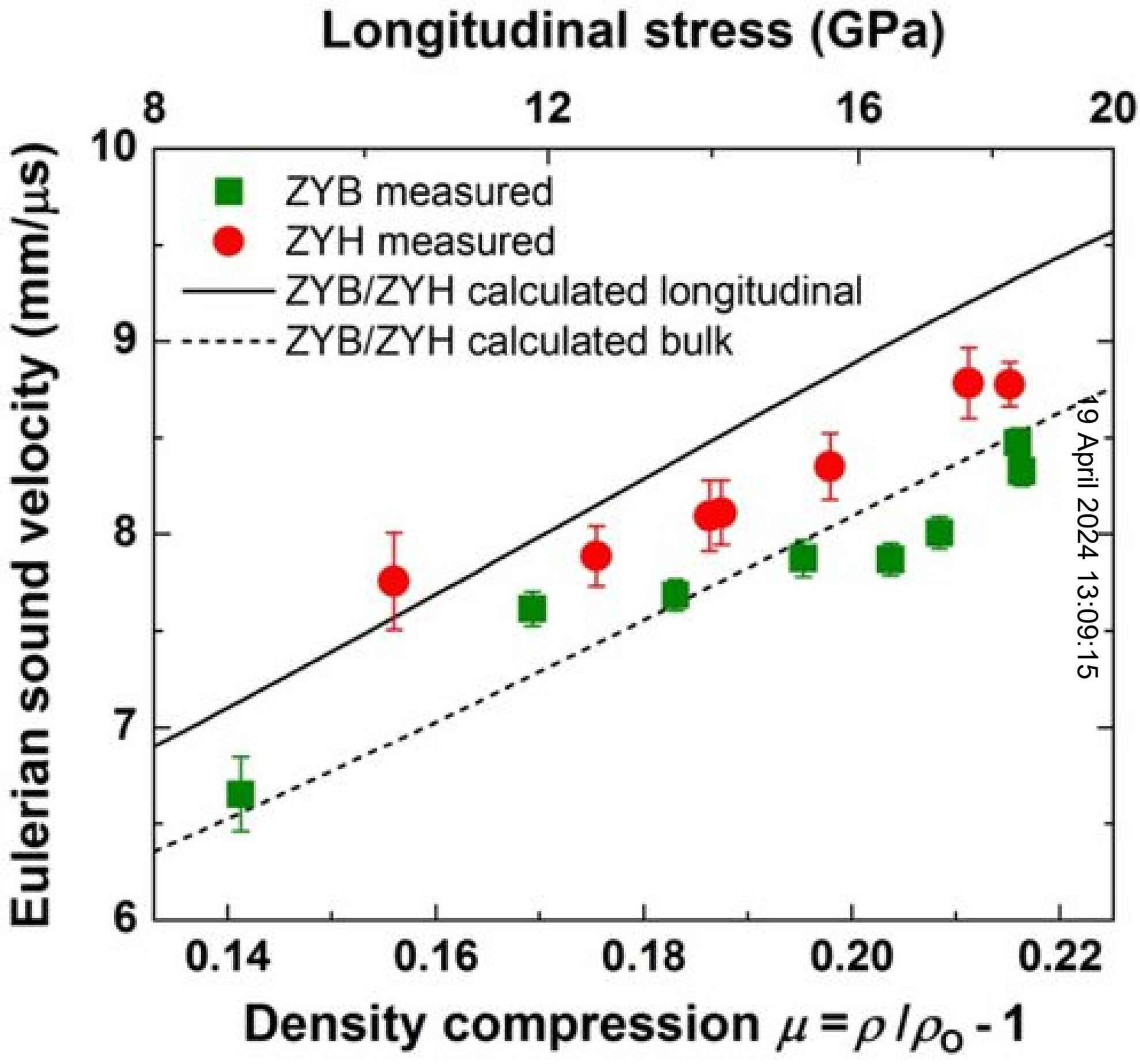

19 April 2024 13:09:15

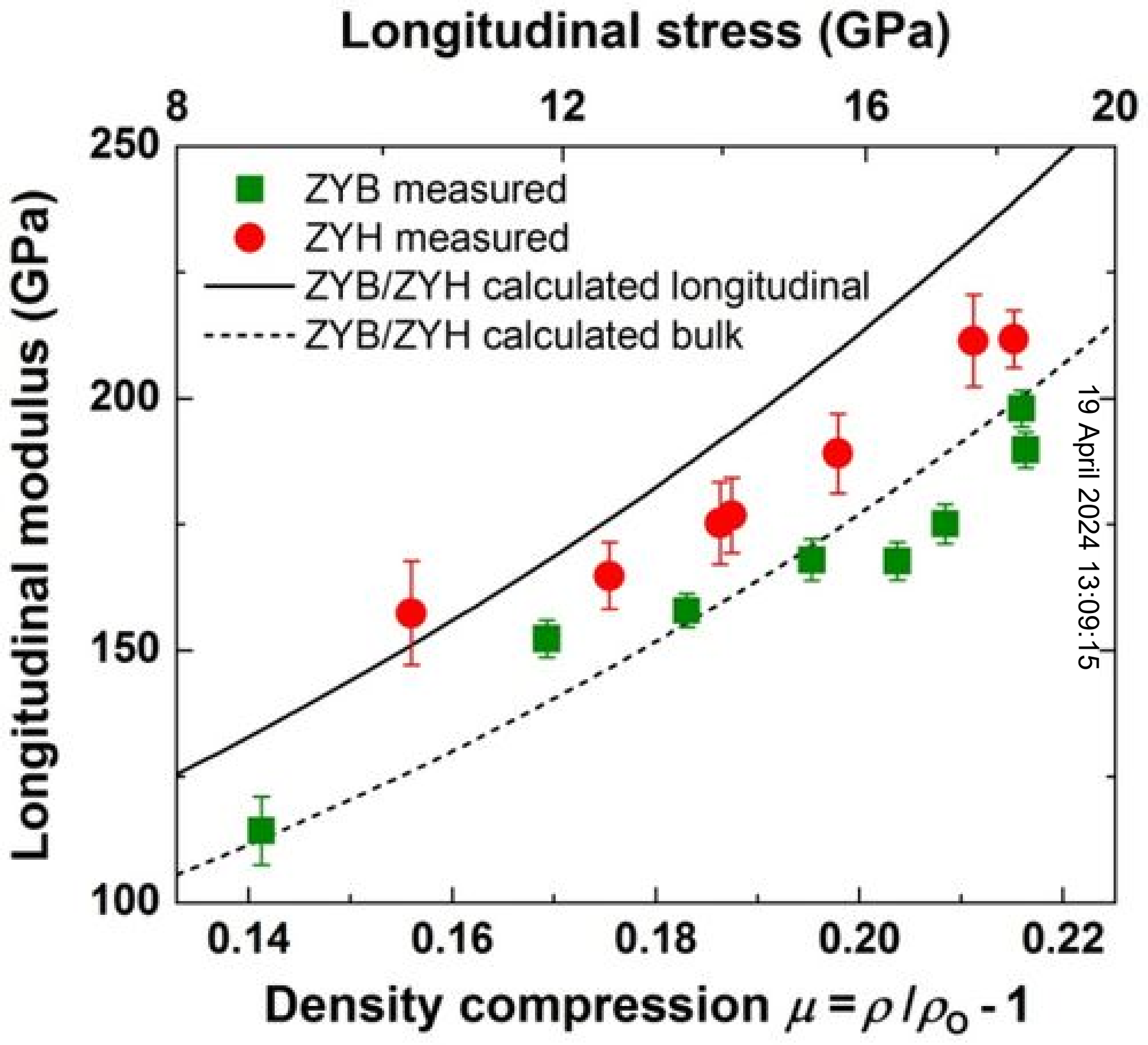
Longitudinal stress (GPa)
8
12
16
20
250
200
150
100
Longitudinal modulus (GPa)
ZYB measured
ZYH measured
ZYB/ZYH calculated longitudinal
ZYB/ZYH calculated bulk
0.14
0.16
0.18
0.20
0.22
Density compression $\mu = \rho / \rho_0 - 1$
19 April 2024 13:09:15